

## Binding of Single Gold Atoms on Thin MgO(001) Films

Maxim Yulikov,<sup>1</sup> Martin Sterrer,<sup>1</sup> Markus Heyde,<sup>1</sup> Hans-Peter Rust,<sup>1</sup> Thomas Risse,<sup>1,\*</sup> Hans-Joachim Freund,<sup>1</sup>  
Gianfranco Pacchioni,<sup>2</sup> and Andrea Scagnelli<sup>2</sup>

<sup>1</sup>*Department of Chemical Physics, Fritz-Haber-Institut der Max-Planck-Gesellschaft, Faradayweg 4-6, D-14195 Berlin, Germany*

<sup>2</sup>*Dipartimento di Scienza dei Materiali, Università di Milano-Bicocca, via R. Cozzi, 53, I-20125 Milano, Italy*

(Received 2 December 2005; published 14 April 2006)

In the present Letter the first electron paramagnetic resonance spectra of single metal atoms on a single crystalline oxide surface are presented. For Au atoms on a MgO(001) film investigated here an analysis of the angular dependent resonance positions and the hyperfine coupling to <sup>17</sup>O shows that the atoms are bound on top of oxygen ions on the terrace of the film. This result is in perfect agreement with scanning tunneling microscopy measurements at 5 K presented here. The measured hyperfine matrix components allow an experimental verification of the theoretically proposed binding mechanism of Au atoms on MgO. In particular, the large reduction of the isotropic hyperfine coupling constant of supported Au as compared to free atoms is not due to a charge transfer at the interface but a hybridization of orbitals and a resulting polarization of the unpaired electron.

DOI: 10.1103/PhysRevLett.96.146804

PACS numbers: 73.20.Hb, 68.37.Ef, 73.20.At, 77.55.+f

A detailed understanding of the properties of supported metal atoms and clusters on insulating surfaces is of paramount importance for a variety of technologically relevant aspects such as heterogeneous catalysis. Gold has come under scrutiny after experiments have unravelled a large catalytic activity of small oxide supported gold clusters with a size of a few nanometers [1,2]. Recently, it was shown that deposited Au clusters of a few atoms change their properties considerably changing their size by single atoms [3]. Therefore, a characterization of the electronic structure of adsorbed metal atoms and small clusters on the supporting oxide surface is a necessary prerequisite to understand these systems on a microscopic level. Even though small clusters and also single metal atoms have been investigated in depth from a theoretical point of view [e.g., [4]], experimental characterization of the electronic structure and binding mechanism of single, supported metal atoms are rather scarce [5]. Electron paramagnetic resonance (EPR) spectroscopy is well suited to investigate these properties as demonstrated for a variety of problems in physics, chemistry, and biology [e.g., [6–11]]. In this Letter the first EPR spectra of single gold atoms on a single crystal oxide surface, using a MgO(001) film as a model surface [12], are presented. In particular, the details of the adsorption site as inferred from the EPR results as well as the impact of the binding on the electronic structure of the Au atoms will be discussed. The former aspect is compared to low-temperature STM measurements, while the latter is discussed in comparison with density functional theory (DFT) calculations, which allows the first direct experimental verification of a theoretically proposed binding mechanism [13]. Finally, hyperfine coupling constants (hfcc) extracted from the experiments will be used to compare with current state of the art DFT calculations.

EPR experiments were performed on a 20 monolayer (ML) thick MgO(001) film grown on a Mo(001) single

crystal. Au atoms were deposited and measured at 30 K. The Mo substrate was cleaned by oxidation with O<sub>2</sub> at 1500 K and subsequent flashes to 2300 K. The MgO films were prepared by deposition of Mg in an oxygen ambient ( $1 \times 10^{-6}$  mbar) at a substrate temperature of 600 K and a rate of 1 ML MgO/min. The films were subsequently annealed to 1100 K for 10 min. The EPR spectra of Au atoms were measured at 30 K with a microwave power of 20 mW in a TE<sub>102</sub> cavity using a modulation amplitude of

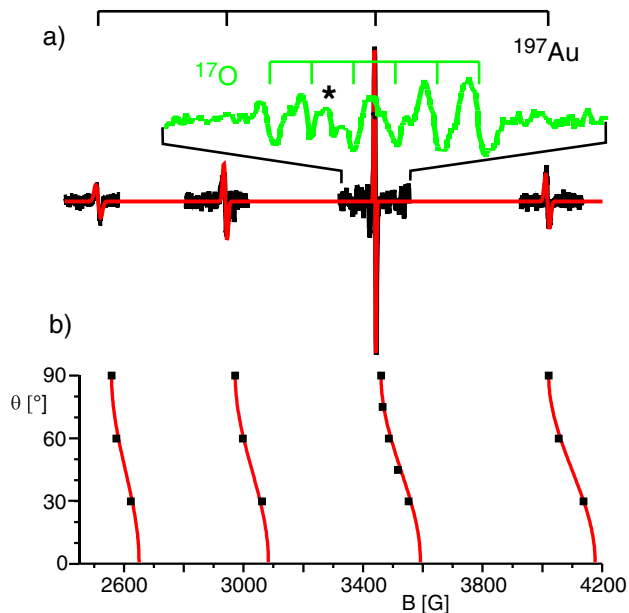


FIG. 1 (color online). (a) Experimental and simulated EPR spectrum of Au atoms adsorbed on MgO(001)/Mo(001) ( $\theta = 90^\circ$ ), green trace: spectrum for an <sup>17</sup>O enriched MgO film (signal marked by a \* belongs to the background). (b) Angular dependence of EPR resonance positions with respect to the polar angle  $\theta$  between static magnetic field and surface normal.

4 G. Details of the experimental setup are described elsewhere [14]. The simulations of the EPR spectra were performed with the EASYPIN package [15]. In addition, STM experiments were carried out in a custom-built low-temperature STM which has been described in detail elsewhere [16]. For the STM experiments a 6–8 ML thick MgO(001) film was grown on Ag(001) by reactive deposition of Mg at 550 K. Au was deposited at 5–8 K. Relativistic all electron DFT calculations using the PW91 exchange-correlation functional were performed using a  $\text{Mg}_{21}\text{O}_{21}$  cluster model embedded in a point charge field. Both spin-polarized scalar relativistic (SR) and spin-restricted calculations with explicit inclusion of spin-orbit effects (SO) have been performed. Hyperfine coupling constants of free and MgO-supported Au atoms as well as for the  $^{17}\text{O}$  ions have been determined using the zero order regular approximation (ZORA) to the Dirac equation as implemented in the Amsterdam density functional (ADF) code [18,19].

Figure 1(a) shows an EPR spectrum after deposition of  $2.8 \times 10^{12}$  Au atoms (0.0025 ML) at 30 K on the MgO(001) film measured with the magnetic field being parallel to the surface. The spectrum consists of 4 resonance lines due to the hyperfine interaction of the electron spin [ $S(\text{Au}) = 1/2$ ] with the nuclear spin of the Au atoms [ $I(^{197}\text{Au}) = 3/2$ , 100% natural abundance; linewidth is between 5 G (most intense line) and 12 G for the low field resonance]. Thus, the observation of the quartet of lines is indicative for the presence of single Au atoms on the MgO surface. The signal intensity corresponds well with a majority of Au nucleating as single atoms. Because of the two-dimensional orientation of the Au atoms it is possible to obtain additional information from angular dependent measurements. Figure 1(b) shows the dependence of the resonance position of the hyperfine quartet with respect to the angle between the static magnetic field and the surface normal. From these angular dependent measurements it is possible to extract the  $g$ - and the hyperfine matrix components as well as their orientation with respect to the surface. The best fit was achieved by assuming axial symmetric  $g$  and  $A$  matrices with  $g_{\parallel} = 1.9904$ ,  $A_{\parallel} = 1410$  MHz and  $g_{\perp} = 2.0652$ ,  $A_{\perp} = 1402$  MHz, where the parallel component is oriented along the surface normal while the other two degenerated components are oriented in the surface plane. The different amplitudes observed for the four hyperfine lines result from a strain in the isotropic hfcc of  $A_{\text{strain}} = 35$  MHz (modeled by a Gaussian distribution  $\sigma = A_{\text{strain}}$ ), which is a consequence of small changes in the local environment for the different adsorption sites. For the present case, hyperfine interaction and Zeeman interaction are of the same order of magnitude. Therefore, the strain has the largest effect on the resonance position at low field, while the smallest effect is found for the third resonance, which explains the difference in signal amplitude.

From these results it is possible to draw two important conclusions concerning (i) the adsorption site of the Au

atoms on the MgO surface and (ii) the redistribution of the electron spin density in the Au atom caused by adsorption onto the oxide surface.

(i) *Adsorption site of Au atoms.*—The adsorption site can be deduced from the orientation of the interaction matrices due to the fact that the local symmetry of the adsorption site has to correspond to the experimental findings. By comparison of the experimental results with expectations for different possible adsorption sites, it turns out that all sites known to be present on the MgO(001) surface (edges, corners, kinks, etc.), except the terrace sites, can be rejected because none of the principle components of the tensor are collinear with the surface normal. However, for the terrace sites the surface normal is a  $C_{4v}$  axis which is collinear with the so-called parallel component of the matrix; thus it is concluded that the atoms are adsorbed on terrace sites of the MgO facets [a more detailed discussion of this point may be found in [9]]. For gold adsorbed on regular MgO terraces theory predicts the atom to be located on top of the oxygen ions [13,20,21]. This can be verified directly by EPR spectroscopy using a film grown with  $^{17}\text{O}_2$  (enrichment 90%). The hyperfine interaction of the unpaired electron with  $^{17}\text{O}$  of the MgO lattice reveals a splitting of each line into six components [see green trace in Fig. 1(a); a small resonance due to the 10% of  $^{16}\text{O}$  is also present; linewidth: 8 G]. This directly confirms one large coupling of the Au atoms to oxygen ions [ $I(^{17}\text{O}) = 5/2$ ]. From the local symmetry and the hyperfine interaction it is concluded that the Au atoms are adsorbed on top of oxygen ions on the terraces of the MgO film.

In parallel low-temperature STM measurements of 0.035 ML, Au adsorbed at 8 K on a nominally 6–8 ML thick MgO(001) film grown on Ag(001) were performed as shown in Fig. 2. Bright spots seen in Fig. 2 are due to single Au atoms adsorbed on the MgO surface. As directly verified from the STM image Au nucleates on the terraces of the MgO surface which is in perfect agreement with the

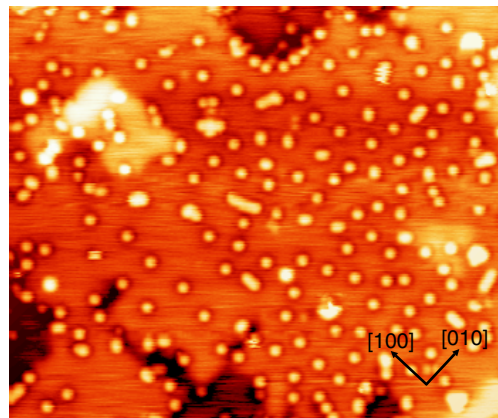


FIG. 2 (color online). STM image ( $30 \times 25 \text{ nm}^2$ ,  $V_S = +0.5 \text{ V}$ ,  $I_t = 10 \text{ pA}$ ) of Au atoms deposited at 8 K on a 6–8 ML thick MgO(001) film grown on Ag(001). The deposited amount of Au atoms corresponds to 0.035 ML.

analysis of the EPR measurements. In addition, 25%–30% of the atoms are nucleated on low symmetry sites (corners, edges, kinks, etc.). These species are not observed in the EPR spectra. This is due to the fact that the symmetry of these sites leads to a large spread of the resonances for the different species. Even for the same species a split may occur due to a lift of degeneracy imposed by the magnetic field. Thus, the individual lines become very weak and cannot be detected with this EPR setup.

(ii) *Hyperfine interaction.*—The hyperfine coupling matrix describing the interaction between the electron spin and the nuclear magnetic moment is governed by two main contributions: the isotropic Fermi-contact term ( $a_{\text{iso}}$ ) and the anisotropic dipolar part ( $\mathbf{T}$ ). Assuming an axial symmetric  $A$  matrix the isotropic part is given by  $a_{\text{iso}} = 1/3(2A_{\perp} + A_{\parallel})$ . It is important to notice that a rigorous deconvolution of the measured hyperfine components into these two parts requires the knowledge of the individual signs of the components, which cannot be determined from the cw-EPR measurements. However, a physically reasonable value for  $a_{\text{iso}}$  is only obtained assuming all components to have the same sign yielding  $a_{\text{iso}} = 1405$  MHz. The components of the traceless dipolar part are then given by  $[-T - T + 2T] = [-2.7 - 2.7 + 5.4]$  MHz. To gain more insight into the change of the electronic structure of the Au atoms upon binding to the MgO surface these values are compared to the corresponding values of free gold atoms [ $a_{\text{iso}}^0(\text{Au}) = 3053$  MHz and  $T_{\text{dip}}^0(\text{Au}) = 26$  MHz] [22]. The isotropic Fermi-contact term is proportional to the electron spin density at the nucleus; thus one can immediately conclude that the spin density at the nucleus is reduced by more than 50% as compared to the free atom. The spin density at the nucleus is governed by the  $6s$  orbital indicating a corresponding reduction of the  $s$  character of the unpaired electron. An even higher reduction, to about 10% of the atomic value, is found for the anisotropic part ( $T$ ) of the hyperfine matrix, which is due to the dipole-dipole interaction of electron and nuclear spin. Since the total spin density is not reduced upon binding for isolated Au atoms, this reduction of the dipolar contribu-

tion can be assigned to an increase of the average distance between the electron spin and the Au nucleus.

A more detailed analysis of the bonding situation can be inferred from comparison with DFT calculations. The bonding between Au and lattice oxygen is very local and has contributions from intraunit polarization but also some covalent character. The latter can either be inferred from the spin density on the oxygen atom [see Fig. 3(a)] or the density of states (DOS) showing a hybridization of the Au  $6s$  level with  $5d$  levels and  $2p$  contributions from the oxygen [13]. The corresponding spin density has not only contributions on the oxygen atom but is also polarized away from the Au atom [see Fig. 3(a)]. These results are perfectly in line with the experimental findings. The hybridization of the  $6s$  level with oxygen  $2p$  and gold  $5d$  levels can account for the reduction of the isotropic hfcc. The same effect leads to a significant spin density on the oxygen atom which is experimentally detected by the  $^{17}\text{O}$  hyperfine coupling constant of 56 MHz for the perpendicular component. This is considerably larger than the coupling observed for K atoms on polycrystalline MgO due to the stronger interaction between Au and the MgO surface; however, the principle mechanism of spin redistribution is very similar in both cases [23]. Finally, this polarization of the oxygen atom in combination with the observed polarization of the spin density away from the Au atom can explain the reduced dipolar contribution. It is important to notice that the reduction of the hfcc compared to the free atom is not a sign of the occurrence of a charge transfer at the Au/MgO interface: the Au atom, in fact, is basically neutral.

From a quantitative point of view Fig. 3(b) shows that  $a_{\text{iso}}$  calculated by DFT scales almost linearly with the distance between Au and the underlying O ion. In case of accurately calibrated DFT results this behavior may be used to extract information about bond distance of Au adsorbed on oxide surfaces indirectly from the measured hfcc. However, the isotropic hfcc calculated for the optimized geometry is slightly below 1700 MHz, which is about 300 MHz larger than observed experimentally. Notice that the inclusion of spin-orbit coupling has little effect, as  $a_{\text{iso}}$  at this level is 1704 MHz. This discrepancy is at variance with calculations for the free atom, which give a value in the range 2939–3124 MHz (depending on the exchange-correlation functional used and on the inclusion of SO effects), much closer to the experimental value of 3058 MHz measured in an atomic beam experiment [24] and 3025–3138 MHz for different matrices [25]. This shows that the method is capable to describe the hfcc of a heavy metal such as Au appropriately. For the oxygen hyperfine interaction a value of  $-70$  MHz (SR) and  $-46$  MHz (SO) is calculated for the perpendicular component of the hyperfine tensor, in reasonable agreement with the observed value of 56 MHz (the sign is not known for the experimental results). A summary of the experimental and theoretical values is found in Table I.

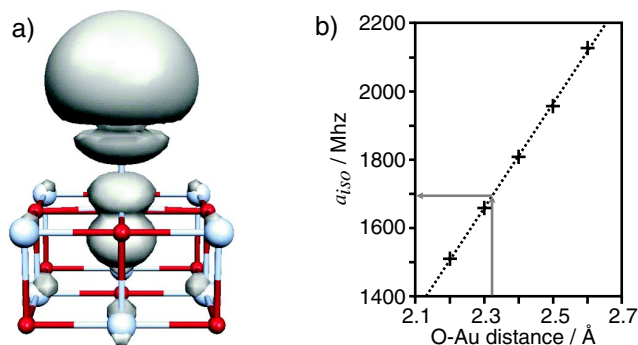


FIG. 3 (color online). (a) Spin density of an Au atom on a MgO terrace. (b) Dependence of the calculated isotropic hfcc of Au adsorbed to terrace sites of the MgO(100) surface on the distance between Au atom and O ion.

TABLE I. Experimental and calculated isotropic and anisotropic hyperfine parameters for free Au atoms and Au atoms supported on MgO as well as  $A_{\perp}$  of  $^{17}\text{O}$  (in MHz).

	$a_{\text{iso}}(\text{Au})$	$T_{\text{dip}}(\text{Au})$	$A_{\perp}(\text{O})$
Free atom experiment [22]	3138	26	
Free atom calculation (SO)	3015		
MgO-supported experiment	1405	2.7	56
MgO-supported calculation (SO)	1704	7.3	-46

It is interesting to discuss the reason for the discrepancy between the calculated and measured values of the isotropic hfcc of MgO-supported Au atoms. The potential for the interaction of Au with MgO is relatively flat. Therefore, small errors in the adsorption energy and in the distance can result in relatively large errors in  $a_{\text{iso}}$ ; see Fig. 3(b). In fact, a reduction of the equilibrium distance by approximately 0.15 Å would account for the observed discrepancy. However, a thorough comparison of a variety of different methods reveals that the minimum geometry is always found between 2.24 and 2.35 Å depending on the method employed [13,20,21]. Thus, additional sources for the discrepancy have to be looked into the approximations of the theoretical approach. First of all, we have considered a point nuclear model. It has been reported that the use of a more realistic finite size of the Au nucleus can have the effect to reduce the hfcc by about 13% [26]. In general, quantitative calculations of hfcc of transition metal systems is still a challenge to quantum chemistry. Core-shell spin polarization and spin contamination are just two effects which contribute to intrinsic uncertainties [27]. Furthermore, small deviations are connected to the choice of the exchange-correlation functional. The combination of all these aspects renders an agreement of the computed hfcc's within 10%–15% of the measured ones satisfactory [27].

In conclusion, we have presented the first EPR spectra of single metal atoms on a single crystal oxide surface. For the present example of Au atoms on a 20 ML thick MgO(001) film on Mo(001) it was possible to determine the adsorption site of the Au atoms, namely, adsorption on top of oxygen ions on the terrace of the MgO surface. This is in good agreement with low-temperature STM measurements. The hyperfine coupling constants measured by EPR spectroscopy are compared to DFT calculations indicating a good qualitative agreement of the theory with the experimental results. In addition, we have shown that the combined use of EPR spectroscopy and DFT calculations of adsorbed Au atoms provides a powerful tool to characterize the nature of the metal-oxide surface bond.

M. S. is grateful for financial support from the Austrian Science Fund. G.P. is grateful to the Alexander von Humboldt Foundation for supporting his visit at the FHI. This work was partially supported by the European Union

through STRP GSOMEN, the NoE IDECAT, and the Fond der Chemischen Industrie.

\*Corresponding author.

Email address: risse@fhi-berlin.mpg.de

- [1] M. Haruta, N. Yamada, T. Kobayashi, and S. Iijima, *J. Catal.* **115**, 301 (1989).
- [2] M. Haruta, *Catal Today* **36**, 153 (1997).
- [3] H. Häkkinen, S. Abbet, A. Sanchez, U. Heiz, and U. Landman, *Angew. Chem., Int. Ed.* **42**, 1297 (2003).
- [4] *Metal Clusters*, edited by W. Ekhardt, Wiley Series in Theoretical Chemistry (Wiley, New York, 1999).
- [5] H.J. Lee, W. Ho, and M. Persson, *Phys. Rev. Lett.* **92**, 186802 (2004).
- [6] S.G. Zech, W. Hofbauer, A. Kamrowski, P. Fromme, D. Stehlik, W. Lubitz, and R. Bittl, *J. Phys. Chem. B* **104**, 9728 (2000).
- [7] B.M. Hoffman, *Proc. Natl. Acad. Sci. U.S.A.* **100**, 3575 (2003).
- [8] K.P. Dinse, *Phys. Chem. Chem. Phys.* **4**, 5442 (2002).
- [9] M. Sterrer, E. Fischbach, T. Risse, and H.-J. Freund, *Phys. Rev. Lett.* **94**, 186101 (2005).
- [10] G. Mitrikas, C. Calle, and A. Schweiger, *Angew. Chem., Int. Ed.* **44**, 3301 (2005).
- [11] S.B. Orlinskii, H. Blok, E.J.J. Groenen, J. Schmidt, P.G. Baranov, C.D. Donegg, and A. Meijerink, *Magn. Reson. Chem.* **43**, S140 (2005).
- [12] M.C. Wu, J.S. Corneille, C.A. Estrada, J.W. He, and D.W. Goodman, *Chem. Phys. Lett.* **182**, 472 (1991).
- [13] A. Del Vitto, G. Pacchioni, F. Delbecq, and P. Sautet, *J. Phys. Chem. B* **109**, 8040 (2005).
- [14] J. Schmidt, T. Risse, H. Hamann, and H.J. Freund, *J. Chem. Phys.* **116**, 10861 (2002).
- [15] S. Stoll and A. Schweiger, *J. Magn. Reson.* **178**, 42 (2006).
- [16] M. Heyde, M. Kulawik, H.-P. Rust, and H.-J. Freund, *Rev. Sci. Instrum.* **75**, 2446 (2004).
- [17] (The following STO all electron basis sets were used: Au [23s15p11d5f]; Mg [7s4p1d]; O [5s3p1d].)
- [18] E. van Lenthe, J.G. Snijders, and E.J. Baerends, *J. Chem. Phys.* **105**, 6505 (1996).
- [19] E. van Lenthe, E.J. Baerends, and J.G. Snijders, *J. Chem. Phys.* **101**, 9783 (1994).
- [20] K.M. Neyman, C. Inntam, V.A. Nasluzov, R. Kosarev, and N. Rösch, *Appl. Phys. A* **78**, 823 (2004).
- [21] G. Barcaro and A. Fortunelli, *J. Chem. Theory Comput.* **1**, 972 (2005).
- [22] D.M. Lindsay and P.H. Kasai, *J. Magn. Reson.* **64**, 278 (1985).
- [23] M. Chiesa, E. Giamello, C. Di Valentin, G. Pacchioni, Z. Sojka, and S. van Doorslaer, *J. Am. Chem. Soc.* **127**, 16935 (2005).
- [24] G. Wessel and H. Lew, *Phys. Rev.* **92**, 641 (1953).
- [25] P.H. Kasai and J.D. McLeod, *J. Chem. Phys.* **55**, 1566 (1971).
- [26] Z.C. Zhang and N.C. Pyper, *Mol. Phys.* **64**, 963 (1988).
- [27] M. Munzarova and M. Kaupp, *J. Phys. Chem. A* **103**, 9966 (1999).